August 2007

Dynamics of tapping mode atomic force microscopy in liquids: Theory and experiments

Sudipta Basak
Birck Nanotechnology Center, School of Mechanical Engineering, Purdue University, sbasak@purdue.edu

Arvind Raman
Birck Nanotechnology Center, School of Mechanical Engineering, Purdue University, raman@purdue.edu

Dynamics of tapping mode atomic force microscopy in liquids: Theory and experiments

Sudipta Basak and Arvind Raman[a)]
Birck Nanotechnology Center and School of Mechanical Engineering, Purdue University, West Lafayette, Indiana 47907-2088

(Received 24 April 2007; accepted 27 June 2007; published online 9 August 2007)

A mathematical model is presented to predict the oscillating dynamics of atomic force microscope cantilevers with nanoscale tips tapping on elastic samples in liquid environments. Theoretical simulations and experiments performed in liquids using low stiffness probes on hard and soft samples reveal that, unlike in air, the second flexural mode of the probe is momentarily excited near times of tip-sample contact. The model also predicts closely the tip amplitude and phase of the tip at different set points. © *2007 American Institute of Physics*. [DOI: 10.1063/1.2760175]

The atomic force microscope (AFM) has become an indispensable tool in biology because it permits the imaging and probing of nanomechanical properties of biological samples such as biopolymers[1,2] and viruses[3] under physiological (liquid environments) conditions. Although the dynamics of the oscillating tip in tapping mode AFM under ambient or ultrahigh vacuum conditions are relatively well understood,[4] very little is known about the tip dynamics in liquid environments.[2,5–9] Here, we present a theoretical model to predict AFM tip dynamics in liquid environments tapping on elastic samples and compare the predictions with experimental results.

We begin by presenting a first-principles mathematical model of the dynamics of the AFM microcantilever vibrating in a viscous, polar fluid and tapping on an elastic surface. The theory is initially developed for uniform, rectangular levers and later extended to levers of arbitrary geometry. The oscillations of the rectangular, uniform cantilever about its equilibrium position then are governed by the following partial differential equation:

$$EIw_{,xxxx} + \rho_c w_{,tt} = f_h + f_d(t) + f_{ts}(Z_c - w(L,t)), \tag{1}$$

where Z_c, $w(x,t)$, f_h, f_d, and f_{ts} are, respectively, the distance of the tip from the surface in the absence of any interaction forces, transverse deflection of the lever, the hydrodynamic forces per unit length due to the surrounding liquid, the driving force, and the tip-sample interaction force. L is the length, EI is the flexural rigidity, and ρ_c is the mass per unit length of the lever.

The tip-sample interaction forces (f_{ts}) are modeled using the Derjaguin-Landau-Verwey-Overbeek (DLVO) theory[10] before contact and by the Derjaguin-Muller-Toporov (DMT) contact mechanics[10] after contact. For the case of a spherical tip and a flat elastic surface this becomes

$$f_{ts}(d) = F_{\mathrm{DLVO}}(d) = \frac{4\pi R_t}{\epsilon\epsilon_0 K_D}\sigma_T\sigma_S e^{-K_D d} - \frac{AR_t}{6d^2}, \quad d \geqslant a_0, \tag{2}$$

$$f_{ts}(d) = F_{\mathrm{DMT}}(d) = \frac{4E'\sqrt{R_t}}{3}(a_0 - d)^{3/2} + F_{\mathrm{DLVO}}(a_0), \quad d < a_0, \tag{3}$$

where E', A, R_t, d, $1/K_D$, ϵ_0, ϵ, σ_T, σ_S, and a_0 are, respectively, effective Young's modulus of the tip and the sample material,[7] the Hamaker constant between the tip and the sample material, the tip radius, the instantaneous tip-sample separation, the Debye length, the permittivity of free space, the dielectric constant of the medium, the surface charge density of the tip and sample, and the intermolecular distance.[11] Neglect of the double layer contribution to the adhesion force leads to a nonphysical force discontinuity at $d=a_0$.[7] Our model includes this contribution and leads to a physically reasonable, continuous interaction model in liquids as supported by prior experimental studies.[12]

Here we focus on a common implementation where the lever is uniformly coated with a magnetic material[1] and excited by an oscillating magnetic field. Accordingly, the magnetic force per unit length is constant over the lever and harmonic in time $f_d(t)=F_d e^{j\omega_d t}$, where F_d is the magnetic force per unit length and ω_d is the drive frequency.

The hydrodynamic forces f_h influence primarily the *Q factors* and *wet resonance frequencies* (resonance frequencies in liquid) of different modes of the lever and can be determined using either fully three-dimensional simulations,[13] or semianalytical hydrodynamic functions close to a sample surface.[14] Alternatively, the Q factors and wet resonance frequencies of each mode close to a surface can be measured experimentally from the thermal spectrum of the cantilever close to the sample surface.

We assume that the cantilever is driven near the resonance frequency of the lowest frequency flexural mode of the cantilever. However, we allow the response to include contributions from the second flexural mode. Accordingly we assume the steady state forced response to be $w(x,t)$

TABLE I. List of levers and substrate materials studied. All samples were investigated with each cantilever. R1, R2, and R3 are rectangular levers and T1 and T2 are triangular levers. L=length, W=width, k=nominal spring constant, and Y=Young's modulus.

Lever	Dimensions $L(\mu m)\times W(\mu m)$	k (N/m)	Substrates	Y (GPa)
R1	250×35	0.2	Polyester	2.8–3.1
R2	300×35	0.15	PVC	2.9–3.4
R3	350×35	0.1	Mica	60
T1	140×18	0.1	Polycarbonate	2–2.4
T2	220×22	0.03	LDPE	0.17–0.28

[a)]Electronic mail: raman@ecn.purdue.edu

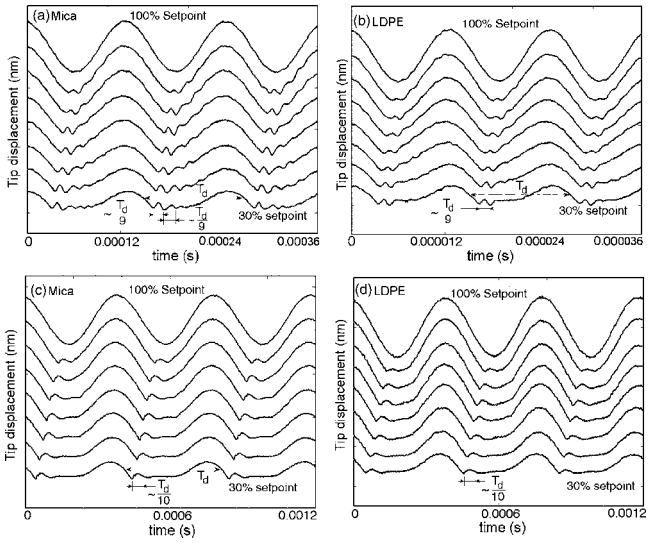

FIG. 1. Tip motion observed in water on mica and LDPE samples for lever R1 (Table I) [(a) and (b)], and for lever T2 (Table I) [(c) and (d)]. For R1, $\omega_d/2\pi=8$ kHz and the amplitude at 100% set point is ~12 nm. For T2, $\omega_d/2\pi=2.5$ kHz and the amplitude at 100% set point is ~12 nm. The wave forms for both levers are acquired from 100% to 30% set point at 10% decrements. Each division on the ordinate axis corresponds to 20 nm.

$=\Psi_1(x)q_1(t)+\Psi_2(x)q_2(t)$, where $\Psi_1(x)$ and $\Psi_2(x)$ are the eigenfunctions of flexural modes 1 and 2 of a cantilever scaled such that $\Psi_1(L)=1$ and $\Psi_2(L)=1$. Furthermore $q_1(t)$ and $q_2(t)$ are the contributions to tip displacement from the two flexural modes, respectively. The absolute tip motion is $q(t)=q_1(t)+q_2(t)$; however, the raw photodiode output is proportional to the slope at the free end of the lever $q_1(t)d\Psi_1(L)/dx+q_2(d\Psi_2(L)/dx)$. The conventional calibration of the photodiode output approximately accounts for the slope of mode 1 only. Thus the conventionally calibrated photodiode output is $q_1(t)+(d\Psi_2(L)/dx/d\Psi_1(L)/dx)q_2(t)$ which equals $q_1(t)+3.47q_2(t)$ for rectangular levers and $q_1(t)+2.69q_2(t)$ for triangular levers (using finite element based modal analysis of typical triangular levers).

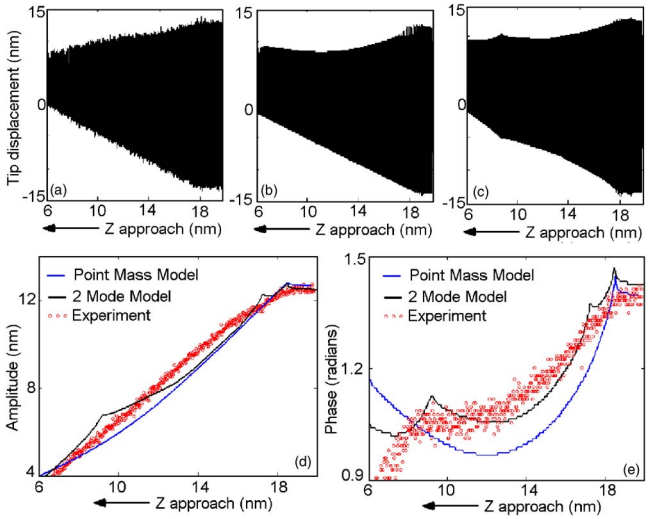

FIG. 2. (Color online) Comparison of experimentally measured and theoretically predicted tip dynamics as lever R1 (Table I) dynamically approaches mica in de-ionized water. The simulation results are obtained by solving Eqs. (4a) and (4b) with zero initial conditions and using interaction and cantilever parameters from Ref. 11. (a) Experimentally measured tip oscillation data, and predictions from (b) the point-mass model, and (c) the two-mode model on mica. Comparison of the point-mass model and the two-mode model with the experimental (d) amplitude-distance and (e) phase-distance plots on mica in water.

Substitution of the hydrodynamic forces by the Q factors and the wet frequencies[13,14] for each mode, inserting $w(x,t)=\Psi_1(x)q_1(t)+\Psi_2(x)q_2(t)$ into Eq. (1), and using the orthogonality relation $\int_0^L\Psi_1(x)\Psi_2(x)dx=0$, we arrive at the following two-degrees-of-freedom tip dynamics model:

$$\frac{q_{1,tt}}{\omega_1^2}+\frac{1}{\omega_1 Q_1}q_{1,t}+q_1=\frac{F_1e^{j\omega_d t}}{k_1}+\frac{f_{ts}(Z_c-q_1-q_2)}{k_1}, \tag{4a}$$

$$\frac{q_{2,tt}}{\omega_2^2}+\frac{1}{\omega_2 Q_2}q_{2,t}+q_2=\frac{F_2e^{j\omega_d t}}{k_2}+\frac{f_{ts}(Z_c-q_1-q_2)}{k_2}, \tag{4b}$$

where $F_1=F_d\int_0^L\Psi_1(x)dx=0.39LF_d$ and $F_2=F_d\int_0^L\Psi_2(x)dx=-0.22LF_d$ are the effective driving forces on modes 1 and 2, respectively. Furthermore, as discussed earlier Q_1, Q_2, ω_1, and ω_2 are the Q factors and the wet frequencies of modes 1 and 2 near the sample surface. The effective stiffnesses of the two modes are given by $k_1=EI(1.875/L)^4\int_0^L\Psi_1^2(x)dx$ and $k_2=EI(4.694/L)^4\int_0^L\Psi_2^2(x)dx$.[15] However, due to inevitable imperfections, these stiffness formulas are approximate, and it is preferable to calculate the effective stiffnesses from experiments using the method of Sader *et al.*[16] Note that by setting $q_2(t)=0$ and retaining only Eq. (4a) we recover the classical *point-mass model* commonly used to model dynamic AFM.[2,5–7] Thus we will compare the theoretically predicted time series for $q_1(t)+(d\Psi_2(L)/dx/d\Psi_1(L)dx)q_2(t)$ with the experimental results which are calibrated conventionally.

Equations (4a) and (4b) have been derived for a uniform rectangular lever. However, they can also be applied to simulate[17] the response of an arbitrarily shaped lever tapping on an elastic sample, in a polar, viscous fluid as long as k_1, k_2, Q_1, Q_2, ω_1, and ω_2 near the sample surface can be determined.

Extensive experiments are performed to measure the tapping tip dynamics in de-ionized water on hard and soft samples and using different types of magnetically excited levers (Table I). The repeatability is excellent. All the experiments are performed on an Agilent 5500 AFM system. The tip displacement data are acquired at a 5 MHz sampling rate using a NI5911 data acquisition board with 16 bit resolution. In this letter we focus on representative experimental results acquired using rectangular lever, R1 and triangular lever, T2 on both mica and soft low density polyethylene (LDPE) samples (Table I). The experimental procedure is as follows: Q_1, Q_2, ω_1, and ω_2 are measured experimentally at a distance of ~15–20 nm from the sample surface. k_1 and k_2 are determined from thermal spectra in air using the method of Sader *et al.*[16] Following this, each probe is magnetically excited at amplitudes of 10–20 nm at a drive frequency corresponding to the maximum resonance amplitude. Next, the tip displacement data are acquired while (i) the tip slowly, continuously approaches the sample, and (ii) the cantilever is held at different positions from the sample; each position leads to a different amplitude reduction or set point amplitude ratio.

We begin by describing a previously unrecognized phenomenon that is observed under all amplitude set points tested and in all cantilever-sample combinations listed in Table I. In Figs. 1(a)–1(d) we present measured tip oscillation wave forms on hard and soft samples that show a dis-

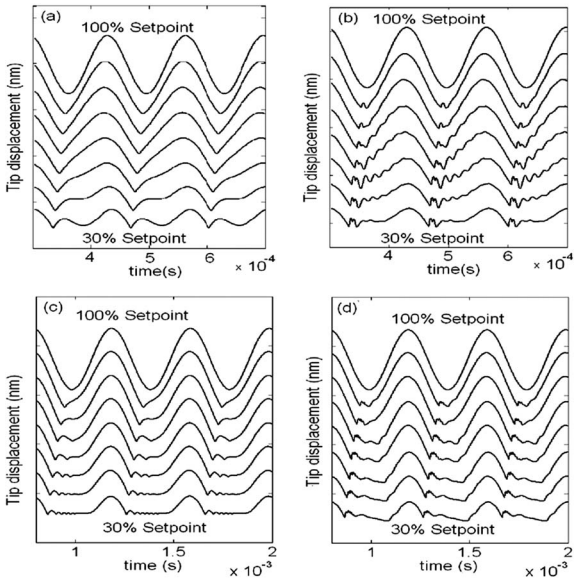

FIG. 3. Theoretically predicted tip displacement history of levers R1 and T2 (Table I) on mica in water as the set point ratio is decreased. (a) Lever R1, point-mass model, and (b) two-mode model; (c) lever T2, point-mass model, (d) two-mode model. The amplitude at 100% set point corresponds to ~12 nm. Tip displacement data from 100% to 30% set point ratio are presented at 10% decrements. The two-mode model predictions match closely with the observed tip displacement data shown in Figs. 1(a) and 1(c).

tinct distortion in the form of decaying ripples of an otherwise harmonic wave near the instants of tip-sample contact. Interestingly, the time period of the localized ripples to that of the driving time period, T_d, *approximately equals* ω_d/ω_2 for all the levers, samples, and set points tested. Moreover, the number of ripples is directly correlated to the Q factor of mode 2 near the sample surface. For instance, the number of ripples for lever R1 (Q_2=6.5) is greater than that for lever T2 (Q_2=2.6). Therefore, the experiments suggest that mode 2 of the cantilever is locally excited near time instants when the tip impacts the sample.

Next we compare the predictions of the two-mode model and the widely used point-mass model[2,5–7] with the experimental results. We focus on the dynamics of levers R1 and T2 on mica for which all the parameters for the numerical simulations are easily determined.[11] The comparisons with data acquired with lever R1 on mica are presented in Figs. 2, 3(a), and 3(b). Clearly the tip-oscillation envelopes, the amplitude, and phase are well predicted by both the point-mass and the two-mode models; the two-mode model predictions are slightly better than those of the point-mass model. However, the tip oscillation wave forms are correctly predicted only by the two-mode model [Fig. 3(b)]. Remarkably, for all set points studied, the two-mode model captures consistently the number and time period of the transient ripples of the second mode near times of tip-sample impact for both levers R1 and T2 [Fig. 3(d)].

The excellent agreement of the two mode model predictions with the experimental tip oscillation wave form [compare Fig. 3(b) with Fig. 1(a) and Fig. 3(d) with Fig. 1(c)] confirms that the tip-sample interaction excites momentarily the second bending mode of the cantilever regardless of the cantilever or sample used. There are two fundamental reasons for this result. First, in liquids the wet frequency f_1 is typically very small (<20 kHz); this means that the higher harmonics in the tapping tip wave form will be spaced narrowly (<20 kHz) apart. Secondly, mode 2 in liquids has a low Q factor so its response bandwidth is wide. As a consequence of both facts, several higher harmonics of the drive frequency will be amplified through nonlinear interactions with the second mode.

The fact that the second vibration mode contributes to the tip dynamics in liquids is an exciting result because studies have suggested that a single mode description is, in most cases, adequate for predicting the tip dynamics in ambient conditions.[18,19] The second mode may significantly influence the tip-sample (imaging) forces and nanomechanical property measurements for applications in liquids and this is a topic of current investigation.

In conclusion we have developed a first-principles model to predict tapping tip dynamics of soft AFM cantilevers on soft and hard elastic samples in liquids. The model uses a physically reasonable tip-sample interaction model, and includes two flexural modes of the cantilever. The proposed model not only correctly predicts this time localized transient behavior but also predicts closely the tip amplitude and phase during approach towards the sample.

The authors acknowledge financial support for this research from the National Science Foundation under Grant No. CMMI 0409660 and from the Sandia National Laboratories under Contract No. 623235.

[1] W. Han, S. Lindsay, and T. Jing, Appl. Phys. Lett. **69**, 4111 (1996).
[2] S. J. T. van Noort, O. H. Willemsen, K. O. van der Werf, B. G. de Grooth, and J. Greve, Langmuir **15**, 7101 (1999).
[3] I. L. Ivanovska, P. J. de Pablo, B. Ibarra, G. Sgalari, F. C. MacKintosh, J. L. Carrascosa, C. Schmidt, and G. J. L. Wuite, Proc. Natl. Acad. Sci. U.S.A. **101**, 7600 (2004).
[4] S. Rutzel, S. I. Lee, and A. Raman, Proc. R. Soc. London, Ser. A **459**, 1925 (2003).
[5] D. Sarid, J. Chen, and R. Workman, Comput. Mater. Sci. **3**, 475 (1995).
[6] G. Y. Chen, R. J. Warmack, P. I. Oden, and T. Thundat, J. Vac. Sci. Technol. B **14**, 1313 (1996).
[7] J. Legleiter and T. Kowalewski, Appl. Phys. Lett. **87**, 163120 (2005).
[8] C. A. J. Putman, K. O. Van der Werf, B. G. De Grooth, N. F. Van Hulst, and J. Greve, Appl. Phys. Lett. **64**, 2454 (1994).
[9] P. K. Hansma, J. P. Cleveland, M. Radmacher, D. A. Walters, P. E. Hillner, M. Bezanilla, M. Fritz, D. Vie, H. Hansma, C. Prater, J. Massie, L. Fukunaga, J. Gurley, and V. Elings, Appl. Phys. Lett. **64**, 1738 (1994).
[10] D. Sarid, *Scanning Force Microscopy*, rev ed. (Oxford University Press, New York, 1994).
[11] The parameters used for the simulation are σ_S (mica)=−0.032 C/m^2, σ_T (SiN)=−0.0025 C/m^2, $1/K_D$ (de-ionized water)=1 μm, A (between mica and Si in water)=3.4×10^{-20} J, E' (between mica and Si)=48.7 GPa, ϵ_0=8.85×10^{-12} F/m, ϵ (de-ionized water)=80, a_0=0.2 nm, and R_t=10 nm. The effective stiffnesses are measured in air, while the Q factors and wet resonance frequencies for modes 1 and 2 used in the simulations are measured experimentally ~15 nm from the surface. These values are determined for lever R1 to be k_1=0.3 N/m, Q_1=2, f_1=8.6 kHz, k_2=10.1 N/m, Q_2=6.5, and f_2=69.4 kHz and for lever T2 to be k_1=0.1 N/m, Q_1=0.6, f_1=2.8 kHz, k_2=3.6 N/m, Q_2=2.6, and f_2=24.8 kHz. The drive frequencies are f_{dr}=8 kHz for lever R1 and f_{dr}=2.5 kHz for lever T2.
[12] B. Cappella, P. Baschieri, C. Frediani, P. Miccoli, and C. Ascoli, IEEE Eng. Med. Biol. Mag. **16**, 58 (1997).
[13] S. Basak, A. Raman, and S. V. Garimella, J. Appl. Phys. **99**, 114906 (2006).
[14] C. Green and J. Sader, Phys. Fluids **17**, 073102 (2005).
[15] J. Melcher, S. Hu, and A. Raman, Appl. Phys. Lett. **91**, 053101 (2007).
[16] J. E. Sader, J. W. M. Chon, and P. Mulvaney, Rev. Sci. Instrum. **70**, 3967 (1999).
[17] These coupled nonlinear equations are simulated using the DDASKR routine with root finding algorithms in FORTRAN, thus ensuring a high degree of accuracy.
[18] T. R. Rodriguez and R. Garcia, Appl. Phys. Lett. **80**, 1646 (2002).
[19] O. Sahin, G. Yaralioglu, R. Grow, S. Zappe, A. Atalar, C. Quate, and O. Solgaard, Sens. Actuators, A **114**, 183 (2004).